Soft Matter

RSC Publishing

REVIEW

Elucidating silk structure using solid-state NMR

Cite this: *Soft Matter*, 2013, **9**, 11440

Tetsuo Asakura,*[a] Yu Suzuki,[a] Yasumoto Nakazawa,[a] Gregory P. Holland[b] and Jeffery L. Yarger*[b]

Received 14th August 2013
Accepted 9th October 2013

DOI: 10.1039/c3sm52187g

www.rsc.org/softmatter

An overview of solid-state NMR structural studies on various silk forms and analogs conducted by the authors' research groups is presented. The well-studied silkworm and spider silks together with related silk peptides have a mixture of secondary structures including β-sheet, β-turn, helix and random coil that are difficult to analyze by X-ray diffraction and electron microscopy but conveniently investigated by solid-state NMR. Several newly developed solid-state NMR techniques and stable isotope labeling approaches of the silks were effectively used to characterize silk structure. The techniques discussed provide not only information on the secondary structure, but also on the hydrogen-bonding interactions present in the silks. Structural studies on other types of silk, silk peptide mimics and recombinant silk proteins are also discussed.

1. Introduction

Recently, considerable attention has been paid to silk by a range of scientists from textile engineers to biochemists and biomedical researchers. Silk is an attractive material because of its excellent mechanical properties, that is, the combinations of strength and toughness not found in today's man-made materials together with excellent biocompatibility.[1] These appealing physical properties originate from the silk fibroin structure and therefore, the atomic level information on the silk structure gives us the answer to why the silk has such excellent properties. X-ray and electron diffraction methods together with other spectroscopic methods have been applied for this purpose. However, silk fibers are inherently non-crystalline or semi-crystalline biopolymers and a mixture of secondary structures including β-sheet, helix, β-turn and random coil are present making silk difficult to analyze by X-ray diffraction and electron microscopy. The conformation-dependent NMR chemical shifts can determine the fraction of mixed structures and monitor the conformational change easily and selectively.[2–4] The techniques discussed provide not only the information on secondary

[a]*Department of Biotechnology, Tokyo University of Agriculture and Technology, 2-24-16, Nakacho, Koganei, Tokyo, 184-8588, Japan. E-mail: asakura@cc.tuat.ac.jp*
[b]*Department of Chemistry and Biochemistry, Magnetic Resonance Research Center, Arizona State University, Tempe, AZ 85287-1604, USA*

Tetsuo Asakura is a Professor of Biotechnology, Tokyo University of Agriculture and Technology. He received his Ph.D. in 1977 in Polymer Chemistry at the Tokyo Institute of Technology. After JSPS Postdoctoral Fellowship, he joined as an Assistant Professor at Nihon University at Matsudo, Department of Dental Materials. In 1981, he became an Associate Professor of Tokyo University of Agriculture and Technology, where he became a full Professor in 1993. From 1990–1991, he worked as a Visiting Professor in Florida State University. His Research has focused on structural analyses of polymers including silk with solid-state NMR and application of silk to biomaterials.

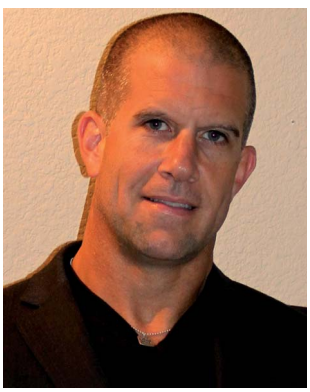

Jeff Yarger received his Ph.D. in Chemistry and Biochemistry in 1996 from Arizona State University (ASU). After a postdoc in the laboratory of Alexander Pines (UC – Berkeley), he obtained an assistant professor position at the University of Wyoming. In 2005, he moved back to ASU and is currently a professor of chemistry, biochemistry and physics as well as the founding director of the Magnetic Resonance Research Center. His research interests are primarily in developing an understanding of the molecular structure and dynamics of soft matter systems including silks, biopolymers, tissues, glasses, polyamorphic and nanoparticle systems for application as advanced materials.

structures of the mixtures, but also on hydrogen-bonding.[3,4] In addition, NMR covers both solution and solid state, including soft matter (or gel state) and further includes looking at silk in living organisms (*e.g.*, silkworms) by solution NMR.[3–5] Furthermore, the atomic level structure can be obtained by using solution or solid-state NMR, by combining with stable ^{2}H, ^{13}C and/or ^{15}N isotope labeling of silks and their sequential model peptides.[1–4] The focus of this review is on the recent solid-state NMR studies used to elucidate the molecular structure of silk fibers and related model peptides.

2. Silkworm silk

Most recently, Zhou's group[6] obtained a single crystal of the N terminal domain of *Bombyx mori* silk fibroin and determined the crystal structure, revealing an entangled β-sheet dimer. However, the structure of the main part, the crystalline domain with the sequence, $(AGSGAG)_n$ is still the target of solid-state NMR. Two crystalline forms of *B. mori* silk fibroin, silk I and silk II, have been reported as the dimorphs of the silk fibroin. Here silk I is the structure of *B. mori* silk fibroin in the solid state obtained from the middle silk gland after drying. The silk II is the structure of *B. mori* silk fibroin fiber after spinning. The structure analyses of silk I and silk II reported by Asakura's group during the past 10 years are reviewed in this section although the structure of another silk protein, silk sericin was also studied with NMR.[7,8]

2.1 Structure of *B. mori* silk fibroin before spinning (silk I) in the solid state

Despite a long history of studying silk I, the structure remained poorly understood because any attempt to induce a macroscopic orientation of the silk sample for X-ray diffraction or electron diffraction analyses, readily caused a conversion of the silk I form to the silk II form.[9] Therefore solid-state NMR is useful because the determination of the silk I structure is possible without orientation or crystallization. The structural features of *B. mori* silk fibroin are conveniently studied by using the synthetic peptide, $(AG)_n$, as a model for the crystalline region[9,10] because the lack of Ser in the model peptide $(AG)_{15}$ does not make any difference in the ^{13}C cross-polarization magic angle spinning (CP-MAS) NMR chemical shifts of the Ala and Gly residues in the repeated sequence $(AGSGAG)_n$ of the native silk fibroin.[11,12]

The backbone structure of the silk I conformation for $(AG)_n$ was determined to be a repeated type II β-turn structure by combining several solid-state NMR techniques, that is, the quantitative use of the conformation dependent chemical shifts, 2D spin diffusion NMR under off magic angle spinning spectra and Rotational Echo Double Resonance (REDOR) experiments for selectively stable-isotope labeled peptides.[13] Namely, by using the ^{13}C chemical shift contour maps for various amino acid residues in the protein as a function of the Φ and Ψ values,[3,4] the Φ and Ψ regions in the Ramachandran map that satisfy both the Cα and Cβ chemical shifts of the Ala residue of $(AG)_{15}$ with silk I form, are determined to be ($\Phi = -80°$ to $-20°$, $\Psi = 90°$ to $180°$). Then the 2D spin-diffusion NMR spectra were observed for $(AG)_6A[1\text{-}^{13}C]G^{14}[1\text{-}^{13}C]$

*Yu Suzuki obtained her Ph.D. in Engineering in 2010 at the Tokyo University of Agriculture & Technology, Japan under the supervision of Professor Tetsuo Asakura on the "NMR Study on the Structures of Repetitive Sequences Characteristic of Silk Fibroin". She obtained an assistant professor position at the Department of Biotechnology, Tokyo University of Agriculture & Technology. She is currently focused on the structural analysis of silk fibroin molecules and functional peptides (*e.g. *metal binding peptides) with solution and solid state NMR.*

Yasumoto Nakazawa obtained his Ph.D. in Engineering in 2003 at the Tokyo University of Agriculture & Technology, Japan under the supervision of Professor Tetsuo Asakura on the "Structural Determination of Silk Fibroin from Wild Silkworms and The Sequential Model Peptides using Nuclear Magnetic Resonance". Throughout his career he has been engaged in structural analysis of fibrous peptide and protein by means of several solid-state NMR techniques. He obtained an associate professor position at the Department of Biotechnology, Tokyo University of Agriculture & Technology.

Greg Holland obtained his Ph.D. in Chemistry in 2003 at the University of Wyoming. After a postdoctoral fellowship at Sandia National Laboratories (Albuquerque, NM), he obtained a research professor position in the Department of Chemistry and Biochemistry and Magnetic Resonance Research Center at Arizona State University, Tempe AZ. His research interests are in NMR spectroscopy with an emphasis on solid, soft matter and liquid-crystalline states including molecular structure and dynamics in biopolymers, biomembranes and nanostructured materials. He is currently focused on studying spider silks, spider venom, lipid rafts, lipid–toxin interactions and biomolecule self-assembly at nanoparticle interfaces.

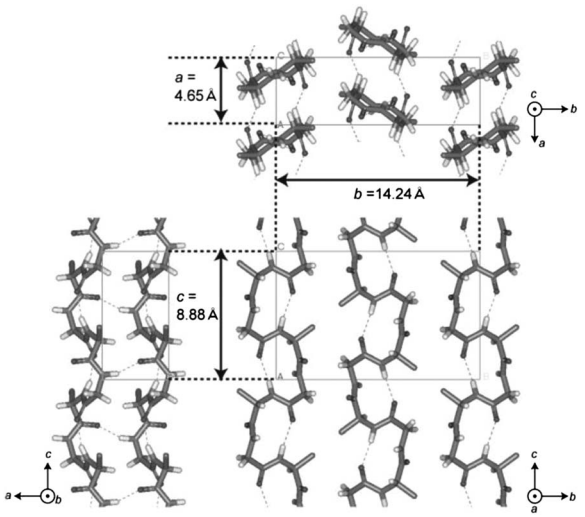

Fig. 1 Repeated type II β-turn structure of $(AG)_{15}$ with intra- and intermolecular hydrogen bonding proposed as the silk I structure.

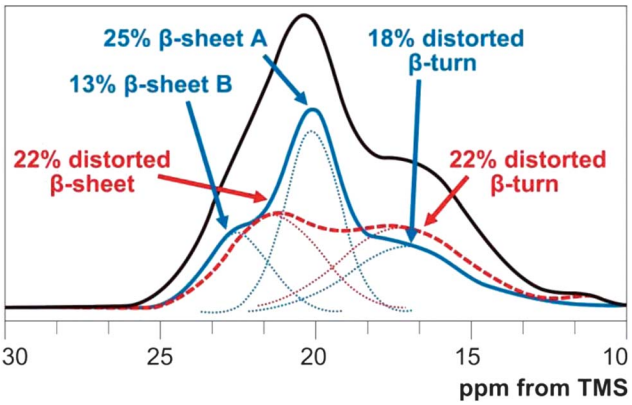

Fig. 2 ^{13}C Ala methyl peak of the ^{13}C CP-MAS NMR spectrum of [3-^{13}C]Ala *B. mori* silk fibroin fiber. The peak was decomposed into the fraction of each conformation.

$A^{15}G(AG)_7$ and $(AG)_7[1\text{-}^{13}C]A^{15}[1\text{-}^{13}C]G^{16}(AG)_7$, to determine the torsional angles of Ala[15] and Gly[16] residues. From the spectral simulation, the torsional angles were determined to be ($\Phi = -60°$ and $\Psi = 130°$) for the Ala residue and ($\Phi = 70°$and $\Psi = 10°$) for the Gly residue. The REDOR experiments to determine the atomic distance between two selectively ^{13}C and ^{15}N double labeled $(AG)_{15}$ were also performed and they supported the structural model for silk I. By adding the structural information from X-ray diffraction analysis of silk I, the final silk I structure forming intra- and inter-molecular hydrogen bonds was proposed as shown in Fig. 1.[14] This structure was also supported by ^{13}C–^{2}H REDOR experiments[15] and ^{1}H solid state NMR.[16]

2.2 Structure of *B. mori* silk fibroin after spinning (silk II)

The structure of silk II has been proposed as a regular array of antiparallel β-sheets firstly by Marsh *et al.*[17] about a half century ago, based on a fiber diffraction study of native *B. mori* silk fibroin fiber. Later, Fraser *et al.*,[18] Lotz *et al.*,[9] and Takahashi *et al.*[19] pointed out some intrinsic structural disorder in the silk II structure although they essentially supported the general features of this anti-parallel β-sheet model. Actually, the Ala Cβ peak in the ^{13}C CP-MAS NMR spectrum of [3-^{13}C]Ala *B. mori* silk fiber in the silk II form is broad and asymmetric, reflecting the heterogeneous structure of the silk fiber (Fig. 2).[20,21] Namely, in the crystalline domain with the sequence, $(AGSGAG)_n$ (solid blue line: 56% of *B. mori* silk fibroin), 18% *distorted* β-turn, 25% β-sheet A and 13% β-sheet B (each is shown as broken blue lines). On the other hand, in the amorphous region (thick broken red line: 44%), the *distorted* β-turn and *distorted* β-sheet are of the same fraction, 22% (each is shown as broken red lines). Takahashi *et al.*[19] proposed two kinds of anti-parallel β-sheet conformation with different inter-molecular arrangements by X-ray diffraction analysis. However, the two β-sheet models by Takahashi *et al.* are unstable with high conformational energies. Thus, a further study is required. Yamauchi and Asakura[22–24] developed a micro-probe with ultra-high speed MAS for high resolution solid-state ^{1}H NMR and used this technique with advanced energy and chemical shift calculations[16] to determine the two β-sheet structures with different inter-molecular arrangements, A and B, in Fig. 2. The structural change from the aqueous solution to silk II was studied with Rheo NMR.[25] The change from silk I film to silk II film by stretching was also studied with solid-state NMR[21] as well as with MD simulation.[26]

3. Spider silk

Spider silk is one of the toughest biopolymers known.[27] Solid-state NMR has played a critical role in determining the molecular structure and dynamics of this proteinaceous fiber. ^{13}C CP-MAS was used to first determine that the poly(Ala) repeat units formed the nanocrystalline β-sheet domains in major[28] and minor[29] ampullate spider silks. Deuterium solid-state NMR was used to probe the molecular orientation and two-component nature of the β-sheet crystalline fraction.[30] Two-dimensional (2D) proton driven spin-diffusion[31] and DOuble Quantum SpectroscopY[32] (DOQSY) solid-state NMR techniques illustrated that the glycine-rich, disordered regions form an approximate 3_{10}-helical conformation. In addition to understanding the backbone conformation and orientation with respect to the fiber axis, solid-state NMR has provided considerable insight into the interaction between spider silk and water and the resulting supercontraction process.[33–38] In this section, we detail the recent (past 5 years) solid-state NMR developments from the Holland and Yarger research groups to elucidate the spider silk structure. Emphasis is placed on the information gained about the spider silk conformational structure and the reader is directed towards a recent review that details the NMR methods used.[4]

3.1 Secondary structure from two-dimensional (2D) solid-state NMR

NMR isotropic chemical shifts provide valuable information regarding the protein secondary structure and have been used since the early 1980's to determine backbone conformation in

silk fibers.[39–41] Although these one-dimensional (1D) ^{13}C CP-MAS NMR methods provide valuable information about the structure, they often have limited resolution because of the broad linewidths observed for silks. The primary amino acid sequences of spider and silkworm silks are highly repetitive where a single amino acid can be present in multiple structural environments. This results in considerable chemical shift heterogeneity that broadens the lines for individual amino acid groups. Recently, two-dimensional homonuclear and heteronuclear solid-state NMR approaches have been used to characterize the secondary structure in ^{13}C- and ^{13}C/^{15}N-istopically enriched spider silks.[42–46] These multi-dimensional, multinuclear NMR techniques yield considerably more structural information compared to the earlier 1D approaches.

An example of a 2D ^{13}C–^{13}C homonuclear correlation spectrum collected with dipolar-assisted rotational resonance[47,48] (DARR) recoupling for ^{13}C-alanine enriched spider dragline silk is presented in Fig. 3.[42] These 2D spectra are collected with various DARR mixing times to probe short- and long-range through-space dipolar contacts between ^{13}C spins. In our experience with moderately (15–50%) ^{13}C-enriched spider silks, intramolecular (within an amino acid) spin connectivity is established with 100–150 ms mixing times, while longer mixing times up to 1 s provide intermolecular (between amino acids) contacts. The 2D ^{13}C–^{13}C correlation spectrum shown in Fig. 3 was collected with a longer recoupling period of 1 s where both intramolecular and intermolecular spatial contacts are observed. These 2D spectra provide two valuable pieces of information not present in the typical 1D ^{13}C CP-MAS spectrum. The first is the ability to extract the distinct carbonyl isotropic chemical shift for the different amino acids by slicing through the low ppm region of the spectrum. The carbonyl isotropic chemical shift provides valuable information regarding the conformational structure and is completely masked in a 1D spectrum where a single, uninformative broad resonance is observed that spans nearly 10 ppm (see Fig. 3a, projection). The second piece of information that the 2D ^{13}C–^{13}C correlation spectrum with a 1 s DARR mixing period provides is the ability to detect long-range intermolecular magnetization exchange between neighboring amino acids. This information can be used to assign specific NMR resonances to the repetitive amino acid motifs present in the spider silk proteins, major ampullate spidroin 1 and 2 (MaSp1 and MaSp2).[49,50] This approach was used to determine that alanine and glycine are both present in two conformational environments, an ordered β-sheet and disordered 3_{10}-helical structure (see Fig. 4a and b). The poly(Ala) and flanking poly(Gly-Ala) repeats in the spider silk proteins form the β-sheet domains while, the Gly-Gly-X motif is present in a 3_{10}-helical structure.

In addition to ^{13}C–^{13}C through-space homonuclear correlation experiments, 2D ^{13}C through-bond double quantum/single quantum (DQ/SQ) correlation spectra collected with the refocused INADEQUATE (incredible natural abundance double quantum transfer experiment) solid-state NMR pulse sequence[51] have also been used to characterize ^{13}C-enriched spider silks.[43–46] The DQ/SQ refocused INADEQUATE experiment greatly improves the resolution by doubling the chemical shift dispersion in the indirect, DQ dimension and has been shown to provide considerable resolution enhancement for disordered solids.[52] For spider silks, the INADEQUATE approach has been used to structurally characterize Tyr in Gly-Gly-X motifs as random coil[45] and the Pro-rich Gly-Pro-Gly-X-X regions unique to MaSp2 as elastin-like, type II β-turns[46]

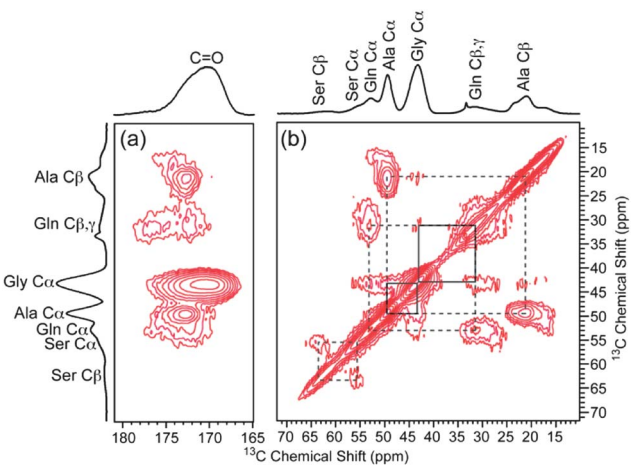

Fig. 3 The 2D ^{13}C–^{13}C correlation spectrum collected with DARR recoupling for ^{13}C-labeled *Nephila clavipes* spider dragline silk. The spectrum was collected at 800 MHz with 40 kHz MAS, a 1 ms CP contact time and 1 s DARR mixing period with $\omega_{RF} = \omega_R$. The (a) high ppm, carbonyl and (b) low ppm regions of the spectrum are shown along with the projections in both dimensions. Intramolecular and intermolecular amino acid contacts are indicated with dashed and solid lines, respectively.

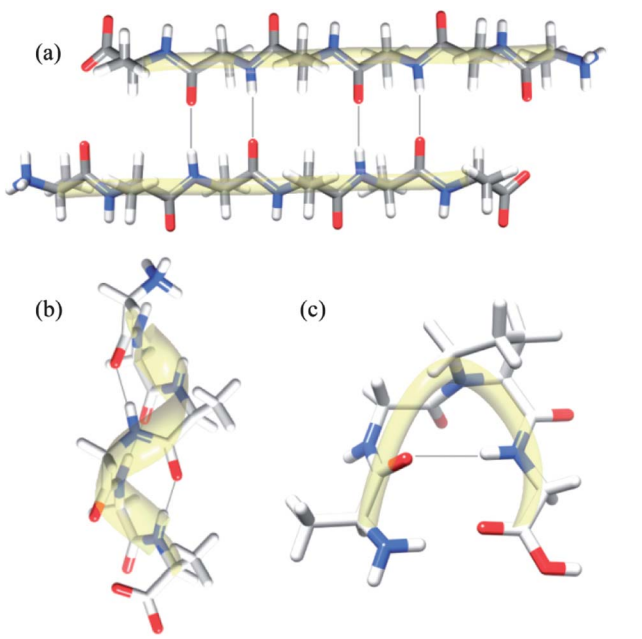

Fig. 4 Secondary structures for the repetitive amino acid motifs found in the spider silk proteins, MaSp1 and MaSp2. Poly(Ala) and poly(Gly-Ala) repeat units present in both proteins form (a) β-sheet structures, the repetitive Gly-Gly-X motif of MaSp1 in a (b) 3_{10}-helical structure and the (c) elastin-like type II β-turn structure for the Gly-Pro-Gly-X-X motif unique to the MaSp2 protein.

(see Fig. 4c). Heteronuclear 2D ^{15}N–^{13}C solid-state NMR spectra collected with double[53] CP (DCP) were used to obtain further structural information from the ^{15}N dimension and confirm that the Pro-rich motifs in spider silk display nearly identical ^{13}C and ^{15}N chemical shifts to those observed for elastin mimics.[46] The presence of elastin-like Pro-containing regions in spider dragline silk helps explain the silk's elongation properties and overall high toughness.

3.2. Quantitative correlation between protein sequence and secondary structure

Utilizing NMR chemical shift assignments and correlations from the 2D through-space ^{13}C–^{13}C correlation spectrum and 2D through-bond ^{13}C–^{13}C refocused INADEQUATE experiments, significant progress has been made in determining the secondary structures of various amino acid motifs that together make up dragline spider silk. Most dragline spider silks are very similar in amino acid composition and overall structure. We have chosen to focus on Black Widow (*L. hesperus*) dragline (major ampullate) silk (BW MA) for quantitative correlation because it is the first and only spider silk that has been fully DNA sequenced (rather than just partial cDNA sequenced, which is available for numerous spider silks).[54,55] For BW MA silk, alanine was determined to be in three distinct secondary conformations, β-sheet, 3_{10}-helix, and α-helix. Proline was ascribed to a β-turn structure. Glycine was found to be in two discrete secondary structures, a β-sheet and a 3_{10}-helix. Additionally, the Gly in a helical conformation was determined to be spatially close to both Ala in a β-sheet and Ala in a helical structure indicating that the helical portion of Gly is an intermediate between the two. Finally, Ser was found to also be in three distinct structures, a β-sheet, helix, and turn. As an example, we show the 2D ^{13}C–^{13}C INADEQUATE NMR spectrum that was used to identify the three Ser structures in Fig. 5.

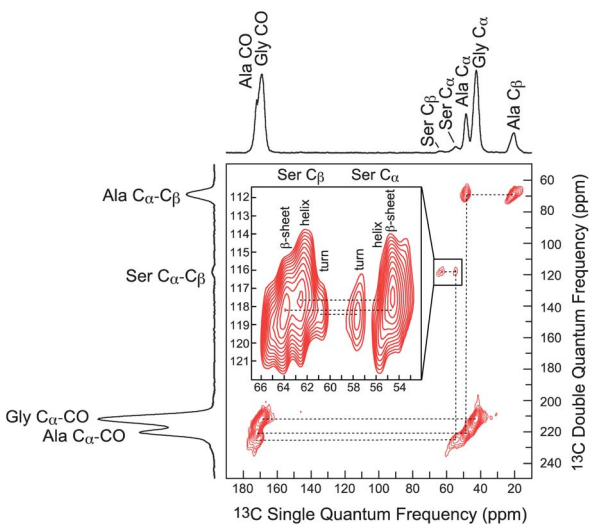

Fig. 5 2D ^{13}C–^{13}C through-bond DQ/SQ refocused INADEQUATE NMR spectrum of U–^{13}C/^{15}N–serine enriched *Latrodectus hesperus* major ampullate (dragline) silk. The three distinct serine resonances are assigned to serine incorporated in three distinct secondary structures, a β-sheet, helix, and β-turn.

These secondary structural assignments were then quantitatively correlated and related to the primary amino acid sequences for both MaSp1 and MaSp2 in BW MA silk. Utilizing solid-state NMR, this study determined that 88% of Ala, 40% of Gly, and 42% of Ser in BW MA silk is incorporated into a β-sheet secondary structure. These values are in good agreement with the predicted values from the primary amino acid sequences of 88%, 42%, and 41% for Ala, Gly, and Ser, respectively. In total, solid-state NMR shows that 47% of all BW MA silk is incorporated into a β-sheet secondary structure. Further comparisons between quantitative NMR and amino acid sequences are underway as this first study to quantitatively correlate the protein sequence and secondary structure in BW MA silk has been very encouraging.

3.3 Hydrogen-bonding from solid-state NMR

Hydrogen-bonding is the primary interaction responsible for the secondary and tertiary structure of proteins. Solution[56] and solid-state[57–62] NMR spectroscopy have played a considerable role in detecting and quantifying hydrogen-bond lengths in small molecules and biopolymers. The advent of very fast (35–40 kHz) and ultra-fast (≥60 kHz) MAS solid-state NMR probes has allowed for improved resolution in the ^{1}H dimension by averaging the strong ^{1}H–^{1}H dipolar interactions in solids with rapid MAS. Sufficient resolution in the ^{1}H dimension is obtained with these rapid MAS rates when the experiments are conducted at high magnetic field strengths (≥600 MHz).[63,64] Recently, the experimental results from fast and ultra-fast MAS ^{1}H NMR spectra have been used in conjunction with theoretical ^{1}H chemical shift calculations to determine hydrogen-bond lengths from amide proton chemical shifts for silk model peptides.[65–67]

2D ^{1}H–^{13}C heteronuclear correlation (HETCOR) solid-state NMR spectra collected with fast MAS were obtained for ^{13}C-labeled spider dragline silk to probe the backbone conformation and hydrogen-bonding from the ^{1}H dimension.[68] The greater chemical shift dispersion of the ^{13}C dimension is required to extract the ^{1}H spectrum in an amino acid specific manner for the spider silk proteins. The ^{1}H spectra extracted for the two Ala Cβ components and the Gly Cα resonance are shown in Fig. 6.

At the intermediate (1 ms) CP contact time used in the ^{1}H–^{13}C HETCOR experiment all proton spins are observed for a given amino acid (*i.e.* Hα, Hβ and NH). The ^{1}H dimension for the two Ala Cβ components displays different Hα chemical shifts where the slices extracted at 21.0 ppm and 17.4 ppm in the ^{13}C dimension display Hα shifts of 5.1 and 4.2 ppm, respectively (see Fig. 6a and b). The observed ^{1}H shifts for the Ala environments agree with previous ^{1}H solid-state NMR on polypeptides where β-sheet structures had shifts of 5.1–5.5 ppm, while helical structures displayed lower shifts of 3.9–4.0 ppm.[69] Thus, the Hα resonance can be used in combination with ^{13}C chemical shifts to characterize the conformational structure in spider silks.

The ^{1}H spectra extracted for both Gly and Ala display two distinct amide proton chemical shifts indicating two

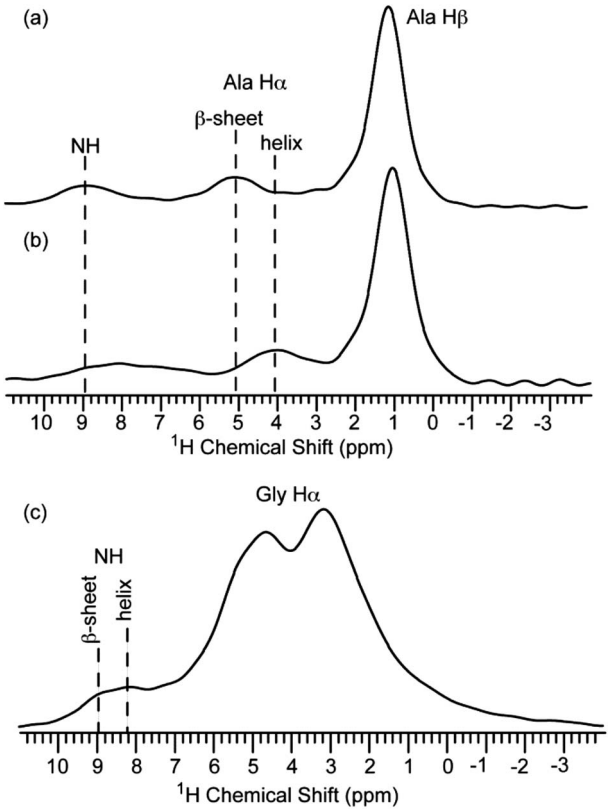

Fig. 6 ^{1}H slices extracted from the 2D ^{1}H–^{13}C HETCOR MAS spectrum of ^{13}C-labled *N. clavipes* dragline silk and specified ^{13}C chemical shifts. Slices obtained at the two Ala Cβ components that correspond to (a) β-sheet (21.0 ppm) and (b) 3_{10}-helical (17.4 ppm) conformations and (c) the Gly Cα (43.3 ppm).

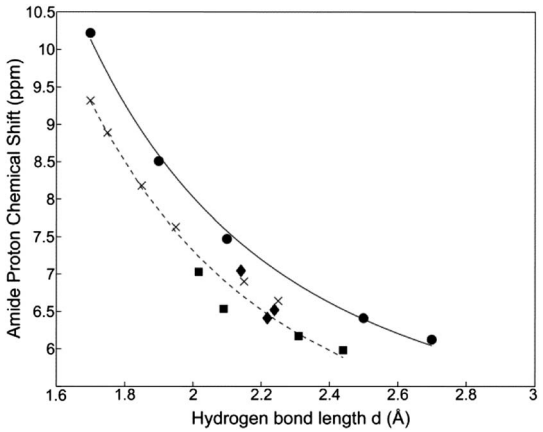

Fig. 7 The calculated amide proton chemical shift (ppm) as a function of NH···OC hydrogen-bond length, *d* (Å). The amide proton chemical shifts were calculated with DFT for (●) β-sheet and helical backbone models. Various helices were used including the (◆) intra-helical and (×) inter-helical hydrogen bonding in a 3_{10}-helix and the (■) intra-helical hydrogen bonding in an ideal α-helix. The calculated data was fit to extract equations for determining NH···OC hydrogen-bond lengths for β-sheet (—) and helical (---) structures from ^{1}H chemical shifts.

hydrogen-bonding environments for both residues (see Fig. 6). The amide proton chemical shift can be dependent on both the hydrogen-bond strength and the backbone conformation. A series of density functional theory (DFT) NMR chemical shift calculations were conducted on model poly(Gly) peptides having β-sheet, 3_{10}-helical and α-helical structures with varying hydrogen-bond lengths to discern the contribution of conformation and hydrogen-bonding.[68] The results of these calculations are presented in Fig. 7. From the DFT calculations, the amide proton chemical shift trend could be determined for β-sheet and helical structures as a function of hydrogen-bond length and the following equations were extracted from the calculated data,

$$\delta_{NH} = 26.8d^{-3} + 4.7, \text{ β-sheet} \quad (1)$$

$$\delta_{NH} = 25.3d^{-3} + 4.1, \text{ helix} \quad (2)$$

where δ_{NH} is the amide ^{1}H chemical shift and *d* is the NH···OC hydrogen-bond distance. Using these equations the hydrogen-bond strength was determined to be equivalent for β-sheet and helical structures in spider silk with a 1.83–1.84 Å NH···OC hydrogen-bond distance.[68] This hydrogen-bond is shorter compared to those previously reported for silk peptide mimics.[66] In addition, this hydrogen-bonding is consistent with inter-strand interactions and provides some of the first pieces of evidence for intermolecular interactions in spider silk.

4. Other silks

While the vast majority of molecular level structural characterization and NMR studies of silk has been done on silkworm and spider silks, silk is a natural protein fiber that is produced by numerous insects and anthropods, both in terrestrial and aqueous environments.[70] Understanding the molecular level differences in silks across a range of species and environments is a critical area where NMR is starting to play a major role. To date, NMR has been used to discern the secondary structure in a number of less studied silks including embiid, caddisfly,[71] hornet,[72] bee,[73] and praying mantis[74] based silk. Most of the NMR to date has been simple ^{1}H–^{13}C CP-MAS solid-state NMR. More informative but complicated NMR can be accomplished, but typically requires isotopic enrichment of ^{2}H, ^{13}C and/or ^{15}N, which presents a lot of individual technical challenges for each species. As an example of silk other than silkworm or spider silk that has been well characterized by NMR, we present a brief summary of NMR data on caddisfly larvae silk, which is spun under water. ^{1}H–^{13}C–^{31}P DCP-MAS solid-state NMR was used to elucidate the molecular protein structure of caddisfly larval silk from the species *Hesperophylax consimilis*. Results provide strong evidence for a structural model in which phosphorylated serine repeats $(pSX)_4$ complex with divalent cations (Fe^{2+}, Ca^{2+} and Mg^{2+}) to form rigid nanocrystalline β-sheet structures. Furthermore, ^{13}C NMR data indicates that both phosphorylated serine and neighboring valine residues exist in a β-sheet conformation, while glycine and leucine residues common in GGX repeats reside in random coil structures. Additionally, ^{31}P chemical shift anisotropy (CSA) analysis shows that the phosphates on phosphoserine residues are doubly ionized, and are charge-stabilized by divalent cations. The resulting model for

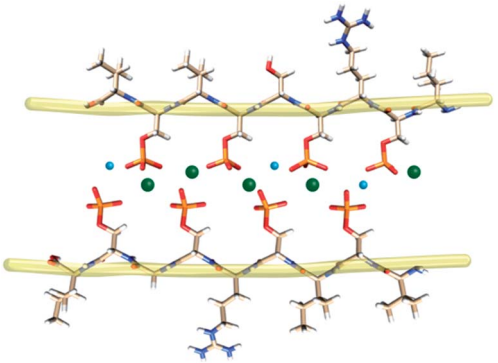

Fig. 8 Proposed structural motif for phosphorylated $(SX)_4$ repeats found in caddisfly silk fibers. In the model, alternating phosphorylated serine residues interact with divalent cations Ca^{2+} and Mg^{2+} to form rigid β-sheet structures. Backbone amide hydrogen bonding would also stabilize sheet formation into and out of the page, thus forming 3-dimensional blocks similar to the poly(Ala) and poly(Gly-Ala) crystalline blocks observed in spider and silkworm silks.

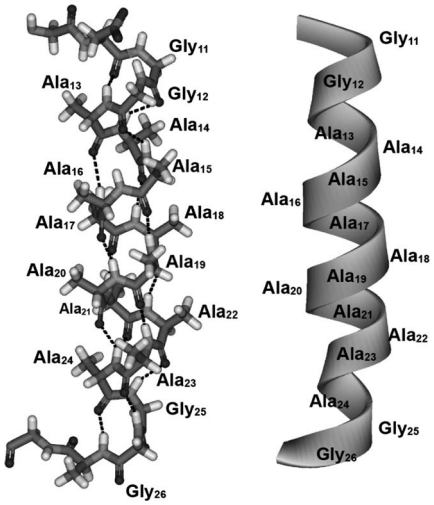

Fig. 9 The helical structure of the poly-Ala region in *S. c. ricini* silk fibroin before spinning. The broken lines indicate intra-molecular hydrogen bondings.

the nanocrystalline β-sheet structures in caddisfly silk is shown in Fig. 8.

Another example of an interesting silk that is being studied by NMR is embiid (webspinners) silk. Individual embiid silk fibers are typically 50–80 nm in diameter and do not contain poly-A or poly-GA motifs like in spider silk and silkworm silk, respectively. In this silk, we find serine-based motifs in nanocrystalline β-sheet domains. Furthermore, this silk is waterproof and the high surface area allows direct observation of the lipids found on the surface of this silk. As NMR has developed as the premier technique for molecular level structural characterization in silkworm and spider silks, it is likely to also become an important characterization tool in all types of terrestrial and aquatic silk materials.

Wild silkworm silks are also interesting. The amino acid composition of silk fibroin from a wild silkworm, *S. c. ricini* and *A. pernyi*,[75,76] is considerably different from that of *B. mori* silk fibroin. The proportion of Gly residues is greater in *B. mori* silk fibroin, while the content of Ala residues is greater in *S. c. ricini* silk fibroin. The solution structure of *S. c. ricini* silk fibroin has been studied with solution ^{13}C and ^{15}N NMR.[77–79] The fast exchange in the NMR time scale between helix and coil forms of the poly(Ala) region has been observed during the helix-to-coil transition with changing temperature. Moreover, solid-state NMR analysis of the ^{13}C-labelled appropriate model peptides leads to the precise silk structure before spinning, where the poly(Ala) sequence takes a typical α-helix pattern with a tightly wound helical structure at both terminal regions of the poly(Ala) sequence. Namely, the 2D spin-diffusion NMR spectra were observed for several [1-^{13}C] double labeled Ala residues in the model peptides. The agreement between observed and simulated spectra is good and therefore the structural model of poly(Ala) sequence is proposed as shown in Fig. 9. The silk fiber after spinning is in a β-sheet structure as determined from the ^{1}H–^{13}C CP-MAS NMR spectrum.

Anaphe is one of the wild silkworms living in equinoctial and southern Africa.[80] Large numbers of the final instar larvae of *Anaphe* form a very large single common silk shell in which individuals then form their own small cocoons. The sequence predominantly contains a mixture of $(AAG)_{n1}$ and $(AG)_{n2}$. The solution and solid state structure were examined with ^{13}C solution and solid state NMR, respectively.[4] The characteristics of the NMR behavior of *Anaphe* silk were between those of *B. mori* and *S. c. ricini* silks.

5. Peptides with silk sequence and recombinant silk protein

The peptides with silk-like sequences are $(AG)_n$ or $(AGSGAG)_n$ for the crystalline domain of *B. mori* silk fibroin and poly(Ala) for *S. c. ricini* and spider silks. In this section, the lamellar structure was proposed for the former peptides, $(AG)_n$ or $(AGSGAG)_n$. For the latter peptides, details of the poly(Ala) β-sheet structure with different inter-molecular structures were discussed. The recombinant silk protein based on these silk sequences and their structural analysis with solid-state NMR were reported. These studies have been performed by Asakura's group for 10 years and applied to biomaterials.

5.1 Lamellar structure of $(AG)_{15}$ with silk II structure

When $(AG)_{15}$ is dissolved in formic acid and then dried, it adopts a silk II antiparallel β-sheet structure. A lamellar structure has been proposed, based on changes in the intensities of asymmetric Ala $^{13}C\beta$ peaks in the ^{13}C CP-MAS NMR spectra coupled with selective ^{13}C labeling of different Ala methyl carbons.[81] As shown in Fig. 10A, the relative intensities of the peaks at 16.7 ppm which were assigned to the distorted β-turn change largely depending on the labeled position of the Ala residue. Therefore the relative intensity was plotted against the residue number of the labeled [3-^{13}C]Ala in Fig. 10B. The plot of the fraction indicates two maxima at the positions, 9 and 19. This implies the appearance of the folded lamellar structure with a β-turn at these positions. Panitch *et al.*[82] reported that

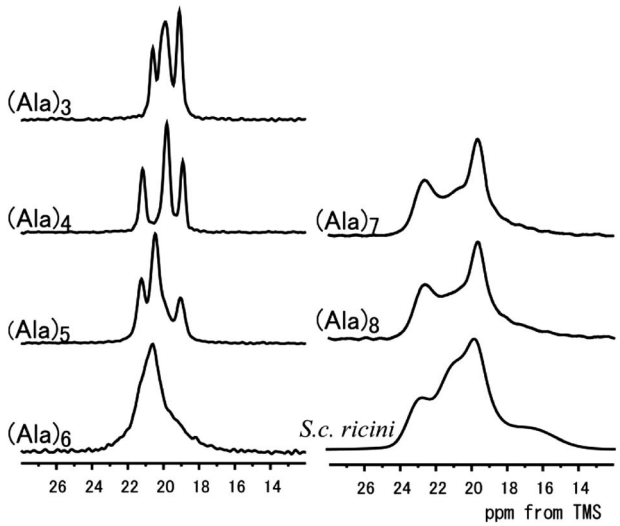

Fig. 10 (A) Expanded Ala Cβ peaks in the ^{13}C CP-MAS NMR spectra of 15 [3-^{13}C](AG)$_{15}$ peptides with different [3-^{13}C]Ala labeling sites. The gray areas are assigned to the distorted β-turn structure. (B) The relative intensity of the 16.7 ppm peak was calculated from these spectra by changing the ^{13}C Ala labeling site in (AG)$_{15}$.

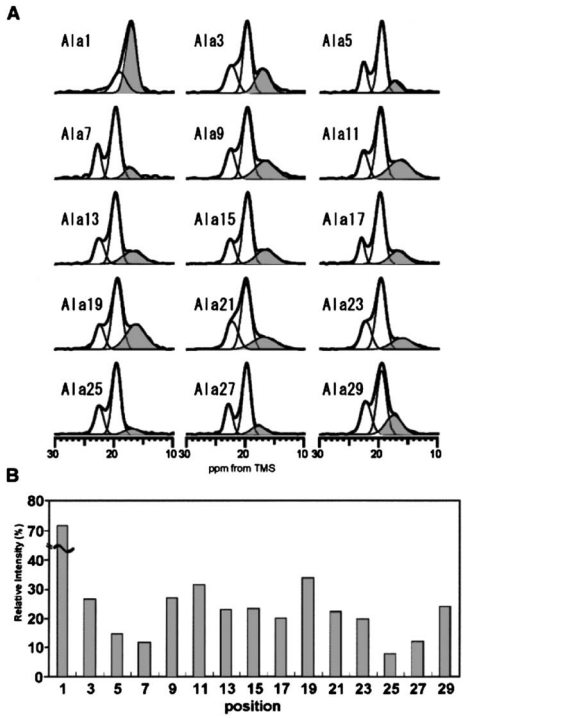

Fig. 11 ^{13}C CP-MAS NMR spectra of (Ala)$_n$ oligomers and *S. c. ricini* silk fibroin (only Ala Cβ regions are shown).

eight amino acid residues contribute to the β-sheet structure for (AG)$_n$ which was studied by X-ray diffraction. This is in agreement with the NMR result. Statistical treatment for the appearance of lamellar structure in (AG)$_{15}$ was also performed.[83] A slightly modified lamellar structure was also proposed for the peptide (AGSGAG)$_n$.[84]

It is interesting to design new silk materials for bone repair scaffold based on the NMR study of the lamellar structure. The silk-like peptides based on AG repeated sequences with a lamellar structure and Asp as a Ca binding site at the turn part were designed and produced in *E. coli.*[85] The lamellar structure formation was confirmed for the model peptide with different ^{13}C labeling positions by solid-state NMR. The surfaces of the recombinant silk protein with the lamellar structure are responsible for calcium binding and accelerated formation of hydroxyapatite. Another *B. mori* silk-like protein, $(E)_n$(AGSGAG)$_4$ where n = 4–8, mimics the primary structure of *B. mori* silk fibroin and were designed and then structurally characterized with ^{13}C solid-state NMR. The balance of hydrophilic and hydrophobic characters of the peptide was controlled by changing the relative length, n, of $(E)_n$ from 4 to 8. Then, genetically modified silk fibroin containing a poly-glutamic acid site for mineralization was produced as fibers by transgenic silkworms,[86] indicating a mineralization-accelerating material for bone repair.

5.2 Polyalanine

Poly(Ala) sequences with β-sheet structure appear frequently in the crystalline regions of spider dragline silk or wild silkworm silks, *S. c. ricini* or *A. pernyi*. The poly(Ala) domains seem to be the origin of the high strength of these silk fibers. Because (Ala)$_3$ can be crystallized in both parallel (P) and antiparallel (AP) β-sheet structures, and the atomic resolution structure was reported by X-ray diffraction studies, this peptide was used to show the usefulness of solid-state NMR including ^{13}C Radio frequency driven recoupling (RFDR), high-field ^{1}H and ^{17}O solid-state NMR and ^{13}C–^{17}O Rotational Echo, Adiabatic Passage, Double Resonance (REAPDOR).[87] Then a systematic NMR analysis of AP poly(Ala) longer than (Ala)$_3$ was performed. In the ^{13}C CP-MAS NMR spectra of (Ala)$_3$, (Ala)$_4$, (Ala)$_5$ and (Ala)$_6$ there is a single central Cβ peak at 20.4 ppm, surrounded by smaller peaks from the two termini (see Fig. 11). In the (Ala)$_6$ spectrum there is also a broad peak at 17.0 ppm, assigned to disordered residues. For (Ala)$_7$ and higher, ^{13}C NMR spectra are markedly different from those for short poly(Ala). NMR shows two Cβ peaks at 22.7 and 19.6 ppm. Line fitting indicated that there is also a third broad peak at about 21.0 ppm, plus the broad peak at 17.0 ppm seen for (Ala)$_6$. It is therefore clear that there is a 'long form' packing, which is different from the 'short form'. With further details from DARR and REDOR experiments for (Ala)$_7$, it is possible to propose a model for the long form. The main difference from the short form is that the packing of chains in adjacent planes is staggered rather than rectangular.[88] High field ^{1}H MAS and ^{15}N CP-MAS NMR were also applied to analyze the structure and hydrogen-bond formation.[67]

5.3 Recombinant silk protein

B. mori silk fibroin can be used for various biomaterial applications. One application is coating the surface of cell culture plates. However, the cell-adhesive ability is weaker than collagen or fibronectin, which are currently used for coating cell culture plates.[3] To increase the biocompatibility of the silk,

recombinant silks that possessed partial collagen or fibronectin sequences, that is, [GERGDLGPQGIAGQRGVV(GER)$_3$-GAS]$_8$GPPGPCCGGG or [TGRGDSPAS]$_8$, respectively were produced by transgenic silkworm.[89] The two types of recombinant silk films possessed a much higher cell-adhesive activity than unmodified silk. Thus, by introducing the cell-adhesive sequence, RGD from fibronectin into silk fibroin by bioengineering techniques, excellent biomaterials have been developed.[89–99] To clarify the origin of such a high cell adhesion character and to design new recombinant silk protein with higher cell adhesion ability, the structure and dynamics of the RGD moiety in a recombinant silk-like protein consisting of the repeated silk fibroin sequence (AGSGAG)$_3$ and the sequence ASTGRGDSPA including the RGD moiety, were studied using NMR.[100] A ^{13}C solid-state NMR study on the ^{13}C selectively labeled model peptide indicates that a random coil state of the RGD moiety is maintained in aqueous solution, and also in both the dry and swollen state. This is similar to the RGD moiety in fibronectin. A novel silk-like protein, [DGG(A)$_{12}$GGAASTGRGD-SPAAS]$_5$, which consists of the poly(Ala) region of silk fibroin from *S. c. ricini*, and cell adhesive region including the RGD sequence was designed and produced.[99] Recombinant proteins with characteristic sequences from the silk fibroin of *Anaphe*, and the cell adhesive region, including the RGD sequence were also designed and produced from *E. coli*.[92] They showed higher cell adhesion activity than *Anaphe* silk fibroin without the RGD sequence. In addition, the activities were very similar to that of collagen, which acted as a positive control. Thus, it is demonstrated that the primary structure of *Anaphe* silk fibroin, which is composed largely of Ala and Gly residues, can be used as a platform for the basic structures of silk-like cell adhesive proteins. The structural characterization of the silk-like recombinant proteins was performed with ^{13}C CP-MAS NMR. The calcium-binding site of the pearl oyster (*Pinctada fucata*) nacreous layer matrix protein MSI60 and calbindin D$_{9k}$ was introduced between different Ala-Gly repeating regions derived from the primary sequences of several silk fibroins.[101,102] The local conformations of the flanking Ala-Gly repeating regions as well as the calcium-binding motif, MSI60, were determined by ^{13}C CP-MAS NMR spectroscopy. The recombinant proteins of silk-elastin and *B. mori* silk-spider silk were also produced and characterized by ^{13}C solid-state NMR.[103,104]

Acknowledgements

T.A. acknowledges support from Grant-in-Aid for Scientific Research from Ministry of Education, Science, Culture and Supports of Japan (23245045,25620169) and Ministry of Agriculture, Forestry and Fisheries of Japan (Agri-HealthTranslational Research Project). GPH and JLY acknowledge support by grants from the Department of Defense (DOD) Air Force Office of Scientific Research (AFOSR) under Award no. FA9550-10-1-0275, the Defense University Research Instrumentation Program (DURIP) under Award no. FA2386-12-1-3031 DURIP 12RSL231 and the National Science Foundation (NSF) Division of Materials Research (DMR) under Award no. DMR-1264801.

References

1 *Biotechnology of Silk*, ed. T. Asakura and T. Miller, Springer, 2013.
2 T. Kameda and T. Asakura, *Annu. Rep. NMR Spectrosc.*, 2002, **46**, 101–149.
3 C. Zhao and T. Asakura, *Prog. Nucl. Magn. Reson. Spectrosc.*, 2001, **39**, 301–352.
4 T. Asakura, Y. Suzuki, Y. Nakazawa, K. Yazawa, G. P. Holland and J. L. Yarger, *Prog. Nucl. Magn. Reson. Spectrosc.*, 2013, **69**, 23–68.
5 T. Asakura, H. Suzuki and Y. Watanabe, *Macromolecules*, 1983, **16**, 1024–1026.
6 Y. X. He, N. N. Zhang, W. F. Li, N. Jia, B. Y. Chen, K. Zhou, J. H. Zhang, Y. X. Chen and C. Z. Zhou, *J. Mol. Biol.*, 2012, **418**, 197–207.
7 H. Teramoto, A. Kakazu and T. Asakura, *Macromolecules*, 2006, **39**, 6–8.
8 H. Teramoto, A. Kakazu, K. Yamauchi and T. Asakura, *Macromolecules*, 2007, **40**, 1562–1569.
9 B. Lotz and F. C. Cesari, *Biochimie*, 1979, **61**, 205–214.
10 K. Okuyama, R. Somashekar, K. Noguchi and S. Ichimura, *Biopolymers*, 2001, **59**, 310–319.
11 J. M. Yao, K. Ohgo, R. Sugino, R. Kishore and T. Asakura, *Biomacromolecules*, 2004, **5**, 1763–1769.
12 T. Asakura, K. Ohgo, T. Ishida, P. Taddei, P. Monti and R. Kishore, *Biomacromolecules*, 2005, **6**, 468–474.
13 T. Asakura, J. Ashida, T. Yamane, T. Kameda, Y. Nakazawa, K. Ohgo and K. Komatsu, *J. Mol. Biol.*, 2001, **306**, 291–305.
14 T. Asakura, K. Ohgo, K. Komatsu, M. Kanenari and K. Okuyama, *Macromolecules*, 2005, **38**, 7397–7403.
15 A. Goldbourt, S. Vega, T. Gullion and A. J. Vega, *J. Am. Chem. Soc.*, 2003, **125**, 11194–11195.
16 T. Asakura, Y. Suzuki, K. Yazawa, A. Aoki, Y. Nishiyama, K. Nishimura, F. Suzuki and H. Kaji, *Macromolecules*, 2013, **46**, 8046–8050.
17 R. E. Marsh, R. B. Corey and L. Pauling, *Biochim. Biophys. Acta*, 1955, **16**, 1–34.
18 B. Fraser and T. P. MacRae, *Conformation of Fibrous Proteins and Related Synthetic Polypeptides*, Academic Press, New York, 1973.
19 Y. Takahashi, M. Gehoh and K. Yuzuriha, *Int. J. Biol. Macromol.*, 1999, **24**, 127–138.
20 T. Asakura, J. Yao, T. Yamane, K. Umemura and A. S. Ulrich, *J. Am. Chem. Soc.*, 2002, **124**, 8794–8795.
21 T. Asakura, R. Sugino, T. Okumura and Y. Nakazawa, *Protein Sci.*, 2002, **11**, 1873–1877.
22 K. Yamauchi, S. Yamasaki, R. Takahashi and T. Asakura, *Solid State Nucl. Magn. Reson.*, 2010, **38**, 27–30.
23 K. Yamauchi, T. Imada and T. Asakura, *J. Phys. Chem. B*, 2005, **109**, 17689–17692.
24 K. Yamauchi and T. Asakura, *Chem. Lett.*, 2006, **35**, 426–427.
25 K. Ohgo, F. Bagusat, T. Asakura and U. Scheler, *J. Am. Chem. Soc.*, 2008, **130**, 4182–4186.
26 T. Asakura, T. Yamane, K. Umemura and Y. Nakazawa, *Macromolecules*, 2003, **36**, 6766–6772.
27 R. V. Lewis, *Chem. Rev.*, 2006, **106**, 3762–3774.

28 A. Simmons, E. Ray and L. W. Jelinski, *Macromolecules*, 1994, **27**, 5235–5237.
29 O. Liivak, A. Flores, R. V. Lewis and L. W. Jelinski, *Macromolecules*, 1997, **30**, 7127–7130.
30 A. H. Simmons, C. A. Michal and L. W. Jelinski, *Science*, 1996, **271**, 84–87.
31 J. Kummerlen, J. D. van Beek, F. Vollrath and B. H. Meier, *Macromolecules*, 1996, **29**, 2920–2928.
32 J. D. van Beek, S. Hess, F. Vollrath and B. Meier, *Proc. Natl. Acad. Sci. U. S. A.*, 2002, **99**, 10266–10271.
33 J. D. van Beek, J. Kummerlen, F. Vollrath and B. H. Meier, *Int. J. Biol. Macromol.*, 1999, **24**, 173–178.
34 L. W. Jelinski, A. Blye, O. Liivak, C. A. Michal, G. LaVerde, A. Seidel, N. Shah and Z. Yang, *Int. J. Biol. Macromol.*, 1999, **24**, 197–201.
35 Z. Yang, O. Liivak, A. Seidel, G. LaVerde, D. B. Zax and L. W. Jelinski, *J. Am. Chem. Soc.*, 2000, **122**, 9019–9025.
36 G. P. Holland, R. V. Lewis and J. L. Yarger, *J. Am. Chem. Soc.*, 2004, **126**, 5867–5872.
37 P. T. Eles and C. A. Michal, *Macromolecules*, 2004, **37**, 1342–1345.
38 G. P. Holland, J. E. Jenkins, M. S. Creager, R. V. Lewis and J. L. Yarger, *Biomacromolecules*, 2008, **9**, 651–657.
39 H. Saitô, Y. Iwanaga, R. Tabeta, M. Narita and T. Asakura, *Chem. Lett.*, 1983, 427–430.
40 H. Saitô, *Magn. Reson. Chem.*, 1986, **24**, 835–852.
41 H. Saito, R. Tabeta, T. Asakura, Y. Iwanaga, A. Shoji, T. Ozaki and I. Ando, *Macromolecules*, 1984, **17**, 1405–1412.
42 G. P. Holland, M. S. Creager, J. E. Jenkins, R. V. Lewis and J. L. Yarger, *J. Am. Chem. Soc.*, 2008, **130**, 9871–9877.
43 G. P. Holland, J. E. Jenkins, M. S. Creager, R. V. Lewis and J. L. Yarger, *Chem. Commun.*, 2008, 5568–5570.
44 J. E. Jenkins, M. S. Creager, R. V. Lewis, G. P. Holland and J. L. Yarger, *Biomacromolecules*, 2010, **11**, 192–200.
45 T. Izdebski, P. Akhenblit, J. E. Jenkins, J. L. Yarger and G. P. Holland, *Biomacromolecules*, 2010, **11**, 168–174.
46 J. E. Jenkins, M. S. Creager, E. B. Butler, R. V. Lewis, J. L. Yarger and G. P. Holland, *Chem. Commun.*, 2010, **46**, 6714–6716.
47 K. Takegoshi, S. Nakamura and T. Terao, *J. Chem. Phys.*, 2003, **118**, 2325–2341.
48 K. Takegoshi, S. Nakamura and T. Terao, *Chem. Phys. Lett.*, 2001, **344**, 631–637.
49 M. Xu and R. Lewis, *Proc. Natl. Acad. Sci. U. S. A.*, 1990, **87**, 7120–7124.
50 M. Hinman and R. V. Lewis, *J. Biol. Chem.*, 1992, **267**, 19320–19324.
51 A. Lesage, M. Bardet and L. Emsley, *J. Am. Chem. Soc.*, 1999, **121**, 10987–10993.
52 D. Sakellariou, S. P. Brown, A. Lesage, S. Hediger, M. Bardet, C. A. Meriles, A. Pines and L. Emsley, *J. Am. Chem. Soc.*, 2003, **125**, 4376–4380.
53 J. Schaefer, R. A. McKay and E. O. Stejskal, *J. Magn. Reson.*, 1979, **34**, 443–447.
54 N. A. Ayoub, J. E. Garb, R. M. Tinghitella, M. A. Collin and C. Y. Hayashi, *PLoS ONE*, 2007, **2**, e514.
55 J. E. Jenkins, S. Sampath, E. Butler, J. Kim, R. W. Henning, G. P. Holland and J. L. Yarger, *Biomacromolecules*, 2013, **14**, 3472–3483.
56 T. K. Harris and A. S. Mildvan, *Proteins*, 1999, **35**, 275–282.
57 B. Berglund and R. W. Vaughan, *J. Chem. Phys.*, 1980, **73**, 2037–2043.
58 G. A. Jeffrey and Y. Yeon, *Acta Crystallogr., Sect. B: Struct. Sci.*, 1986, **42**, 410–413.
59 R. K. Harris, P. Jackson, L. H. Merwin, B. J. Say and G. Hagele, *J. Chem. Soc., Faraday Trans. 1*, 1988, **84**, 3649–3672.
60 I. Schnell, S. P. Brown, H. Y. Low, H. Ishida and H. W. Spiess, *J. Am. Chem. Soc.*, 1998, **120**, 11784–11795.
61 D. H. Zhou and C. M. Rienstra, *Angew. Chem., Int. Ed.*, 2008, **47**, 7328–7331.
62 J. W. Blanchard, T. L. Groy, J. L. Yarger and G. P. Holland, *J. Phys. Chem. C*, 2012, **116**, 18824–18830.
63 A. Samoson, T. Tuherm and Z. Gan, *Solid State Nucl. Magn. Reson.*, 2001, **20**, 130–136.
64 D. H. Zhou, G. Shah, M. Cormos, C. Mullen, D. Sandoz and C. M. Rienstra, *J. Am. Chem. Soc.*, 2007, **129**, 11791–11801.
65 K. Yamauchi, S. Kuroki, K. Fujii and I. Ando, *Chem. Phys. Lett.*, 2000, **324**, 435–439.
66 K. Yazawa, F. Suzuki, Y. Nishiyama, T. Ohata, A. Aoki, K. Nishimura, H. Kaji, T. Shimizu and T. Asakura, *Chem. Commun.*, 2012, **48**, 11199–11201.
67 Y. Suzuki, R. Takahashi, T. Shimizu, M. Tansho, K. Yamauchi, M. P. Williamson and T. Asakura, *J. Phys. Chem. B*, 2009, **113**, 9756–9761.
68 G. P. Holland, Q. Mou and J. L. Yarger, *Chem. Commun.*, 2013, **49**, 6680–6682.
69 A. Shoji, H. Kimura, T. Ozaki, H. Sugisawa and K. Deguchi, *J. Am. Chem. Soc.*, 1996, **118**, 7604–7607.
70 T. D. Sutherland, J. H. Young, S. Weisman, C. Y. Hayashi and D. J. Merritt, *Annu. Rev. Entomol.*, 2010, **55**, 171–188.
71 J. B. Addison, N. N. Ashton, W. S. Weber, R. J. Stewart, G. P. Holland and J. L. Yarger, *Biomacromolecules*, 2013, **14**, 1140–1148.
72 T. Kameda, *Polym. J.*, 2012, **44**, 876–881.
73 T. Kameda and Y. Tamada, *Int. J. Biol. Macromol.*, 2009, **44**, 64–69.
74 A. A. Walker, S. Weisman, T. Kameda and T. D. Sutherland, *Biomacromolecules*, 2012, **13**, 4264–4272.
75 H. Sezutsu and K. Yukuhiro, *J. Mol. Evol.*, 2000, **51**, 329–338.
76 J. Magoshi, Y. Magoshi and S. Nakamura, *J. Appl. Polym. Sci.*, 1977, **21**, 2405–2407.
77 Y. Nakazawa and T. Asakura, *FEBS Lett.*, 2002, **529**, 188–192.
78 T. Asakura and T. Murakami, *Macromolecules*, 1985, **18**, 2614–2619.
79 T. Asakura, H. Kashiba and H. Yoshimizu, *Macromolecules*, 1988, **21**, 644–648.
80 H. Akai and T. Nakashima, *Int. J. Wild Silkmoth Silk*, 1999, **4**, 13–16.
81 T. Asakura, Y. Nakazawa, E. Ohnishi and F. Moro, *Protein Sci.*, 2005, **14**, 2654–2657.

82 A. Panitch, K. Matsuki, E. J. Cantor, S. J. Cooper, E. D. T. Atkins, M. J. Fournier, T. L. Mason and D. A. Tirrell, *Macromolecules*, 1997, **30**, 42–49.
83 T. Asakura, H. Sato, F. Moro, Y. Nakazawa and A. Aoki, *J. Am. Chem. Soc.*, 2007, **129**, 5703–5709.
84 Y. Suzuki, A. Aoki, Y. Nakazawa, D. P. Knight and T. Asakura, *Macromolecules*, 2010, **43**, 9434–9440.
85 T. Asakura, H. Sato, F. Moro, M. Y. Yang, Y. Nakazawa, A. M. Collins and D. Knight, *Macromolecules*, 2007, **40**, 8983–8990.
86 A. Nagano, Y. Tanioka, N. Sakurai, H. Sezutsu, N. Kuboyama, H. Kiba, Y. Tanimoto, N. Nishiyama and T. Asakura, *Acta Biomater.*, 2011, **7**, 1192–1201.
87 T. Asakura, M. Okonogi, Y. Nakazawa and K. Yamauchi, *J. Am. Chem. Soc.*, 2006, **128**, 6231–6238.
88 T. Asakura, M. Okonogi, K. Horiguchi, A. Aoki, H. Saito, D. P. Knight and M. P. Williamson, *Angew. Chem., Int. Ed.*, 2012, **51**, 1212–1215.
89 S. Yanagisawa, Z. H. Zhu, I. Kobayashi, K. Uchino, Y. Tamada, T. Tamura and T. Asakura, *Biomacromolecules*, 2007, **8**, 3487–3492.
90 J. Yao and T. Asakura, Silks, in *Encyclopedia of Biomaterials and Biomedical Engineering*, ed. G. E. Wnek and G. L. Bowlin, Marcel Dekker, Inc., NY, 2004, pp. 1363–1370.
91 M. Yang, C. Tanaka, K. Yamauchi, K. Ohgo, M. Kurokawa and T. Asakura, *J. Biomed. Mater. Res., Part A*, 2008, **84**, 353–363.
92 C. Tanaka and T. Asakura, *Biomacromolecules*, 2009, **10**, 923–928.
93 T. Tamura, C. Thilbert, C. Royer, T. Kanda, E. Abraham, M. Kamba, N. Komoto, J. L. Thomas, B. Mauchamp, G. Chavancy, P. Shirk, M. Fraser, J. C. Prudhomme and P. Couble, *Nat. Biotechnol.*, 2000, **18**, 81–84.
94 L. Meinel, V. Karageorgiou, S. Hofmann, R. Fajardo, B. Snyder, C. M. Li, L. Zichner, R. Langer, G. Vunjak-Novakovic and D. L. Kaplan, *J. Biomed. Mater. Res., Part A*, 2004, **71**, 25–34.
95 L. Meinel, S. Hofmann, V. Karageorgiou, C. Kirker-Head, J. McCool, G. Gronowicz, L. Zichner, R. Langer, G. Vunjak-Novakovic and D. L. Kaplan, *Biomaterials*, 2005, **26**, 147–155.
96 U. Hersel, C. Dahmen and H. Kessler, *Biomaterials*, 2003, **24**, 4385–4415.
97 E. S. Gil, B. B. Mandal, S. H. Park, J. K. Marchant, F. G. Omenetto and D. L. Kaplan, *Biomaterials*, 2010, **31**, 8953–8963.
98 J. S. Chen, G. H. Altman, V. Karageorgiou, R. Horan, A. Collette, V. Volloch, T. Colabro and D. L. Kaplan, *J. Biomed. Mater. Res., Part A*, 2003, **67**, 559–570.
99 T. Asakura, C. Tanaka, M. Y. Yang, J. M. Yao and M. Kurokawa, *Biomaterials*, 2004, **25**, 617–624.
100 T. Asakura, H. Nishi, A. Nagano, A. Yoshida, Y. Nakazawa, M. Kamiya and M. Demura, *Biomacromolecules*, 2011, **12**, 3910–3916.
101 T. Asakura, M. Hamada, Y. Nakazawa, S.-W. Ha and D. P. Knight, *Biomacromolecules*, 2006, **7**, 627–634.
102 T. Asakura, M. Hamada, S. W. Ha and D. P. Knight, *Biomacromolecules*, 2006, **7**, 1996–2002.
103 K. Ohgo, T. L. Kurano, K. Kumashiro and T. Asakura, *Biomacromolecules*, 2004, **5**, 744–750.
104 M. Y. Yang and T. Asakura, *J. Biochem.*, 2005, **137**, 721–729.

